Structural Health Monitoring Issues Using Inclinometers on Prestressed Concrete Girder Bridge Decks

Structural Health Monitoring Issues Using Inclinometers on Prestressed Concrete Girder Bridge Decks

To cite this article: Gabriele Bertagnoli *et al* 2021 *IOP Conf. Ser.: Mater. Sci. Eng.* **1203** 032101

Structural Health Monitoring Issues Using Inclinometers on Prestressed Concrete Girder Bridge Decks

Gabriele Bertagnoli[1], Costanza Anerdi[1], Mario Ferrara[1]

[1] Politecnico di Torino, Corso Duca degli Abruzzi, 10129, Turin, Italy

gabriele.bertagnoli@polito.it

Abstract. In the last decades, assessment and rehabilitation of the existing built environment constitute one of the major challenges for engineers, practitioners and code-makers all over the world. Aging, deterioration processes, lack of or improper maintenance, and increasing occurrence of extreme events have led to the need of more efficient methods for the safety assessment and retrofitting/rehabilitation of existing concrete structures like bridges. New approaches deriving from research should be able to provide solutions devoted to reduce and/or avoid the necessity of interventions, verifying the safety conditions for human life and performances for serviceability on aged infrastructures. Structural Health Monitoring (SHM) of existing bridges has become a key issue in all western world as most of the infrastructures of each Country are reaching the end of their design life. SHM can be divided classically in two approaches: static and dynamic. Static SHM is based on the measure of displacements and their derivatives like rotations or strains regardless of the dynamic behaviour of the structure. Clinometers are among the most used devices to measure angles on structures; they can provide high accuracy when used in static mode as advanced techniques of signal processing can be used to reduce the noise of the signal working on acquisitions that can last several seconds to provide one single accurate measure of angle. Nevertheless, many issues one the affidability and the correct use of measures done with clinometers have to be addressed to achieve a trustworthy SHM using such devices. In this paper the most relevant issues related to the f.e.m. modelling of a bridge deck in view of the use of clinometers for SHM are presented providing explanation using a test case bridge that has been under continuous investigation for many months. A brief explanation of the process for data cleaning and interpretation is also given, stressing out the limits of the technology and the possible outcomes.

1. Introduction

Most Western World countries built their backbone infrastructures after WWII between 1950 and 1980. This heritage of roads, railways and highways bridges and tunnels is nowadays becoming old and it is often suffering serious deterioration problems [1] [2].

During the last ten years, the evolution of low cost sensors derived from TLC industry, the development of broadband internet communication, the rise of cloud based services and the growth of big data platforms, have changed the scenario of Structural Health Monitoring (SHM) that can now be deployed on large scale to infrastructures as a standard option and not only when specific pathologies are found [3] [4] [5] [6] [7].

This paper presents the studies and the tests done before the use of a Structural Health Monitoring (SHM) system on a prestressed bridge deck. Prestressed bridge decks are, in fact one of the most objects of concern for structural safety nowadays [8] [9] [10] [11].

The SHM system is made of high precision clinometers, it was installed before the beginning of repair and strengthening works and it has been active on the bridge deck for several months during repair operations. Traffic has been kept open on the deck during repair by means of carriageways reduction.

The initial test and calibration of the SHM system is done by means of the application of a static load in absence of traffic: four lorries are placed on one side of the deck to maximize the torque effect and therefore the bending action on the most external longitudinal beam.

A finite element model (f.e.m.) is developed to be used during the continuous monitoring phase to provide mechanical interpretation to the data coming from the monitoring system.

The geometry of the deck is taken from the original blueprints and the material properties are known from a widespread test campaign on several specimens taken from the deck.

The f.e.m is calibrated in order to fit the deformed shape of the deck measured by the clinometers during the load test done before the beginning of the monitoring activity.

The f.e.m. model is calibrated with a refinement procedure in order to understand which structural mechanisms and characteristics are playing a major role in determining the deformation of the deck under service variable loads.

The study starts with a simple f.e.m. model and step by step increases the complexity until a good accordance with measured data is achieved.

The basic characteristics of the f.e.m. model is the need to be as simple as possible and easy to be created using standard commercial softwares or even self-written f.e.m. codes, like the one developed in Python for this application. It should be simple as it may be used quickly to provide real time interpretation to the monitoring data. The development of a f.e.m. Phyton code is therefore intended to a possible future application of this code directly on the Raspberry Pi [12] used in the sensors control unit installed by the bridge.

A sensitivity study of the design choices leading to the best accordance between numerical model output and load test data are presented in order to help designer in their modelling choices when dealing with SHM of girder deck bridges.

2. Bridge deck description

The monitored bridge is part of a highway. It has been built between 1967 and 1969, it is made of several isostatic decks with a span of 45m and a width of 19.1m.

Each deck is made of six longitudinal beams and four transverse beams as can be seen in **Figure 1** and in **Figure 2**. The top slab is 20cm thick, the cross section of the longitudinal and the transverse beams is shown in **Figure 3**. The transverse cross section is saddlebacked as both carriageways are supported by the same deck; the two central beams are at the same level, whereas each beam is 20cm lower moving towards the edge of the deck (see **Figure 2**).

Each longitudinal beam of the deck is prestressed using 94 prestressing strands with 93mm^2 cross section each; 70 strands are straight running at the bottom of the beam and 24 are deviated upwards at the extremities of the beams to reduce prestressing moment. One post tensioning bonded tendon made of 32ϕ7 wires with a total cross section area of 1232mm^2 is also present with a parabolic curve from the bearing to 15m and then a linear layout at the bottom of the beam until midspan.

A throughout testing campaign on the materials was done taking from the deck: twelve cylindrical specimens ϕ=94 h=94 mm from the beams and six specimens with the same dimensions from the slab, nine ordinary reinforcements bars segments (3ϕ8, 3ϕ10 and 3ϕ16), five pre-stressing strands segment and five wires from the post-tensioning tendon. The mean material properties obtained by testing these specimens are given in **Table 1**.

Table 1. Mean material properties

			Beams	Slab
Concrete cylindrical compressive strength	fc	[MPa]	57	49
Concrete Young modulus	Ec	[GPa]	37.0	35.3
Ordinary reinforcement yielding strength	fy	[MPa]	425	
Prestressing strands tensile strength	fpt	[MPa]	1819	
Post tensioning tendon tensile strenght		[MPa]	1700	

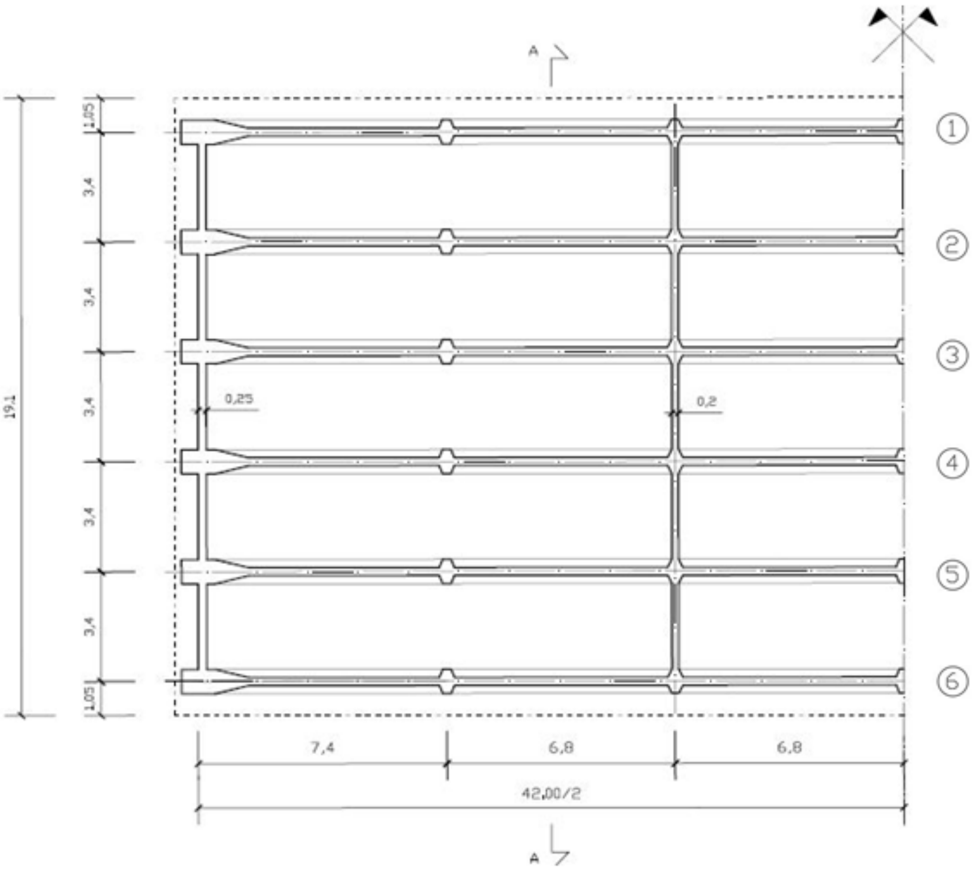

Figure 1. Half girder plan view

The deck is instrumented with eight self-compensated mems clinometers placed at the extremities of the internal beams (beams 2 to 5): four on the north side and four on the south side.

The characteristics of the instruments declared by the producer are: sensor resolution 0.00056°, reading frequency 2 Hz, stability at 20 days under repeated conditions in laboratory < 0.007°, accuracy ±0.002°, temperature dependency (-20°<T<+70°C) ±0.002° / °C, 32 bit A/D converter. Tiltmeters were mounted on 2m long aluminium bars in order to measure the mean rotation of the first 2 meters of each beam.

3. Initial load test description

After the installation of the monitoring system the deck has been statically tested using four lorries weighting 34t each. The position of the lorries on the deck, their shape and their weight on each tire is given in **Figure 4**.

IOP Conf. Series: Materials Science and Engineering 1203 (2021) 032101 doi:10.1088/1757-899X/1203/3/032101

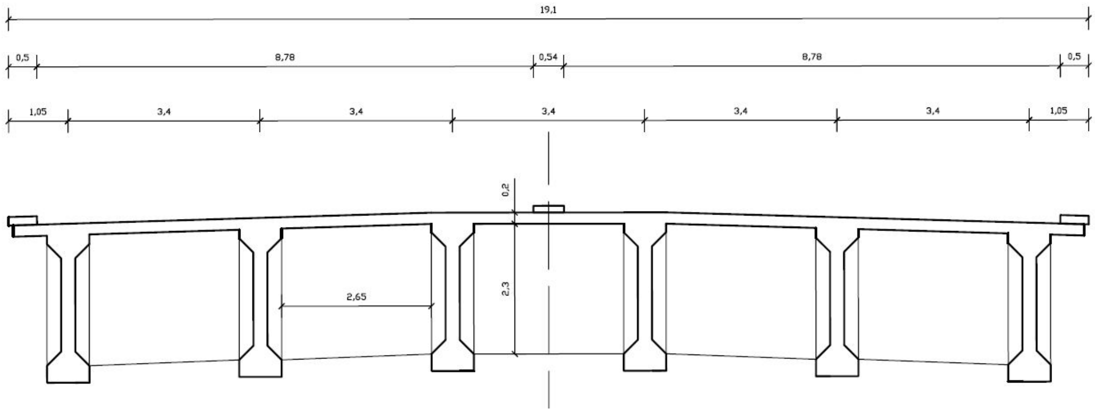

Figure 2. Girder transverse cross section

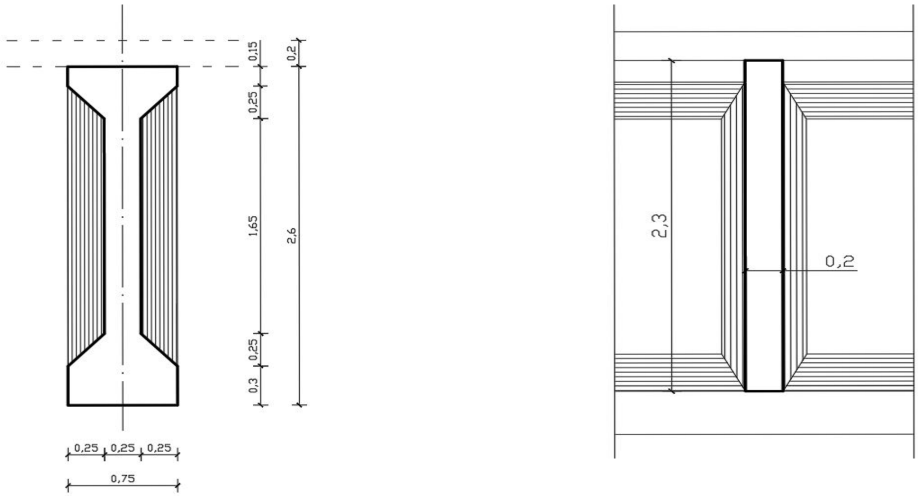

Figure 3. Longitudinal and transverse beams cross section

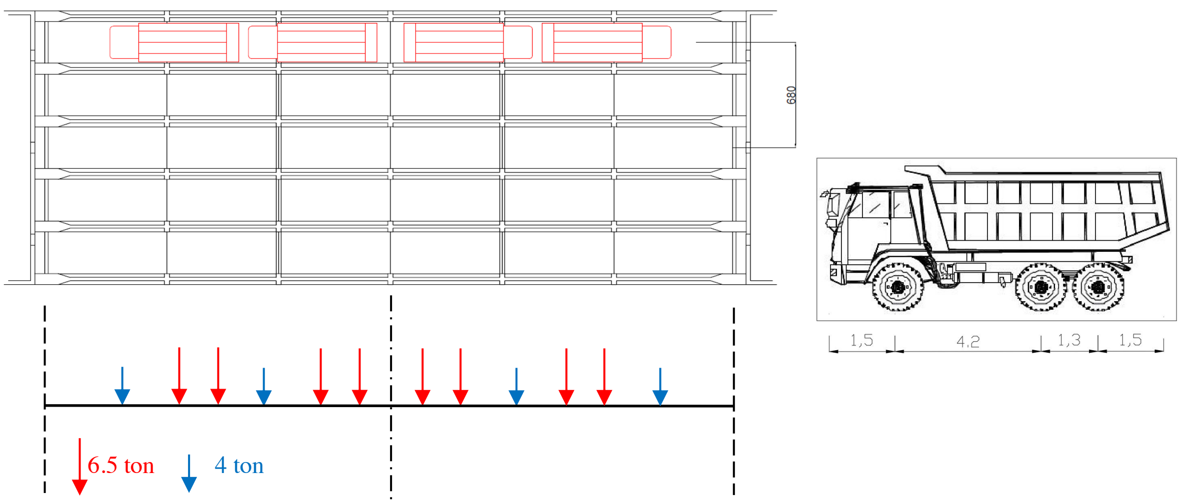

Figure 4. Lorries silhouette and position during test

4. Finite element models of the deck and load test results comparison

The deck was modelled using simple 3D beams elements [13]. The collaborating width of the slab is calculated according to paragraph 5.3.2.1 of EN 1992-1-1 for all beams [14].

Two different cross sections for longitudinal beams were used. The first, assigned to external (edge) beams, includes 2.75m of top slab that is eccentric with respect to the web axis because the width of the kerb is smaller than the interaxis between longitudinal beams. The second, assigned to internal beams, includes 3.4m of centred top slab that is exactly the interaxis between longitudinal beams.

Also two different sections for transverse beams were used. The first, assigned to the first and the fourth transverse beams (the ones connecting bearings), includes only 1.4m of top slab because the effective span of these elements is only the interaxis of 3.4m between longitudinal beams. The second section is assigned to the two central transverse beams and includes 6.33m of top slab. The effective span of these beams is indeed taken equal to 17m that is the transverse distance between the two external longitudinal beams. This assumption is very important as the stiffness of these two transverse beams is highly dependent on the amount of collaborating slab. The effective span of a beam is related to the distance between the points where the bending moment is nil. If the longitudinal beams are considered as elastic supports for the transverse one, the deflection of the transverse beam is characterized by a curvature of the same sign along the whole transverse for most load positions. Therefore the effective span can be even wider than the distance between the two external longitudinal beams in many cases. In the present work it has been approximated to 17m as if the transverse beam was simply supported on the two external beams.

The comparison between the results of the simplified models, realized with 3D beams and described in this paragraph, and the ones obtained using a more refined finite element model, realized using shells and 3D brick elements, has proved the correctness of this choice and the effectiveness of more than 6m of slab working with the web of the transverse beam.

The remaining part of the slab, which is not taken into account as the top flange of the transverse beams is then divided into stripes of about one meter of width and modelled as transverse slab stripes as can be seen in Figure 5. The cross section properties of all the elements are shown in Table 2. Plain concrete properties are calculated taking into account only the difference between slab and beams concrete grade, whereas homogenized properties are calculated taking into account the presence of reinforcement and prestressing. Homogenization is done with respect to the Young modulus of the concrete of the beams.

Table 2. Cross section properties

	Plain concrete section				Homogenized section			
	A [m^2]	Iy [m^4]	Iz [m^4]	I_T [m^4]	A_0 [m^2]	Iy_0 [m^4]	Iz_0 [m^4]	I_{T0} [m^4]
Longitudinal external beams	1.550	0.409	1.567	0.0342	1.580	0.417	1.680	0.0344
Longitudinal internal beams	1.680	0.680	1.676	0.0350	1.710	0.691	1.790	0.0352
Slab stripe (1.01m)	0.203	1.76E-2	6.8E-4	2.36E-3	0.209	1.79E-2	7.0E-4	2.38E-3
Transverse internal beams	1.726	4.230	0.734	0.134	1.775	4.30	0.771	0.138
Transverse external beams	0.855	0.050	0.548	0.126	0.875	0.052	0.576	0.127

Several different models have been developed in order to test the level of accuracy needed to obtain the same deformed shape measured during the load test described in paragraph 3.

According to design blueprints, the north side of the deck is provided with fixed bearings in longitudinal direction whereas the south side has free rollers realized by means of double pendulum bearings. No specification is given on the bearings behaviour in transverse direction, but at they were supposed to act as fixed ones. The role of the bearings and the type of the reaction they can transfer plays a fundamental role in the behaviour of the deck under serviceability conditions, like the one represented by the load test. The importance of this parameter will be discussed in the following.

The first bearing layout hypothesis adopted in fem models is presented in **Table 3**.

Table 3. Restrained degrees of freedom in bearings

Bearing	N1 to N2	N3	N4 to N6	S1 to S2	S3	S4 to S6
F longitudinal	Fixed	Fixed	Fixed	Free	Free	Free
F transverse	Free	Fixed	Free	Free	Fixed	Free
F vertical	Fixed	Fixed	Fixed	Fixed	Fixed	Fixed
Rx Ry Rz	Free	Free	Free	Free	Free	Free

On north side al bearings are fixed in longitudinal direction and only one is fixed in transverse direction. On south side all bearings are free in longitudinal direction and only one is fixed in transverse one. Beam nr.3 has been chosen to get the transverse fixed one. Results do not change if another beam is chosen. During load test no horizontal load are applied, therefore the only horizontal forces that may occur in the bearings are related to the compatibility of the deformation of the deck.

The horizontal displacements in transverse direction caused by the

The rotations obtained in each model, loaded with the load pattern shown in Figure 4, is compared to real one measured on the bridge during the load test in Table 4. The rotations measured during the test are not perfectly symmetric (north values differs from south ones) even if the deck should theoretically assume a symmetric behaviour. Rotations obtained by f.e.m. models are symmetric (north = south) as the models and the applied loads are symmetric. The difference between numerical values and experimental one is expressed in Table 4 as a percentage with respect to the rotation of beam 2, which shows the biggest deformation; a range a÷b is given as the calculation is done both for north and south experimental values.

The first model, pictured in Figure 5 (a), is perfectly flat and does not take into consideration the vertical eccentricities among beams, slab, and bearings. This kind of model was commonly used for the design of such kind of decks in the past 20 years as it is simple and it benefits from reduced input time.

The results obtained by this model overestimate the deformability of the deck of about 26% on the most deformed instrumented beam.

The second model, pictured in Figure 5 (b), differs from model (a) only because of the introduction of the vertical offsets between the centroids of longitudinal and transverse beam and top slab. The results are similar to the ones obtained with model (a), just a little bit stiffer, registering a maximum overestimation of the deformability of 24%.

The third model is based on the geometry with offsets used in the second but cross sectional properties of beams and slab are calculated taking into account of homogenization due to effective reinforcement bars and prestressing strands and tendons layout. The variation due to homogenization is shown in Table 2. The results are stiffer than the ones obtained with model 2, reducing the maximum difference to about 16%.

The fourth model is derived from the third by introducing the transverse saddlebacked slope appreciable in Figure 2. No significative difference is appreciated between the results obtained using model 3 and model 4.

The fifth model introduces in model 4 the vertical offsets of the bearings positions as shown in Figure 5 (d). The vertical elements that are connecting the bearings to the centroids of the longitudinal beams are 1.76m long and are modelled with a cross section of 0.75 by 1.0m trying to represent the deformability of the web of the longitudinal beams that are 0.75m thick at the beginning of the deck as shown in Figure 3. This modification slightly increases the stiffness of the deck, providing the results given in Table 4.

The new correct position of the bearings asks for a correction of the model of the external transverse beams. In order to model the transverse restraint offered by it also at the level of the bearings, the 1st and 4th transverse beam are split into two elements, as can be seen in Figure 5 (e). The inertia properties of the T shaped transverse are divided between the two elements in order to maintain the global stiffness unchanged. This modification increases the overall stiffness reducing the maximum error to 9÷12%.

As the results of model 6 are still quite far from the measured ones, the authors decided to introduce a non-linear behaviour within the bearing devices to take into account the friction in free bearings.

The north side of the deck is fixed in longitudinal direction, as shown in Table 3, therefore no friction effect is considered, but the south side ha free longitudinal bearings for all six beams until model 6. In model 7 a friction coefficient in longitudinal direction equal to 5% is introduced in all south bearings.

The bearing behaviour is rigid (until maximum horizontal force allowable by friction is reached) then perfectly plastic. This means that the static friction force is maintained during sliding, ignoring the reduction between static and sliding friction coefficient, or, seeing if from a different point of view, applying a 5% sliding friction and underestimating the friction one by considering equal to the sliding one. The vertical reaction in each bearing due to permanent loads is equal to 1170 kN (simplifying hypothesis of equal reaction in all bearings is assumed). An example of friction forces is shown in Figure 5 (f).

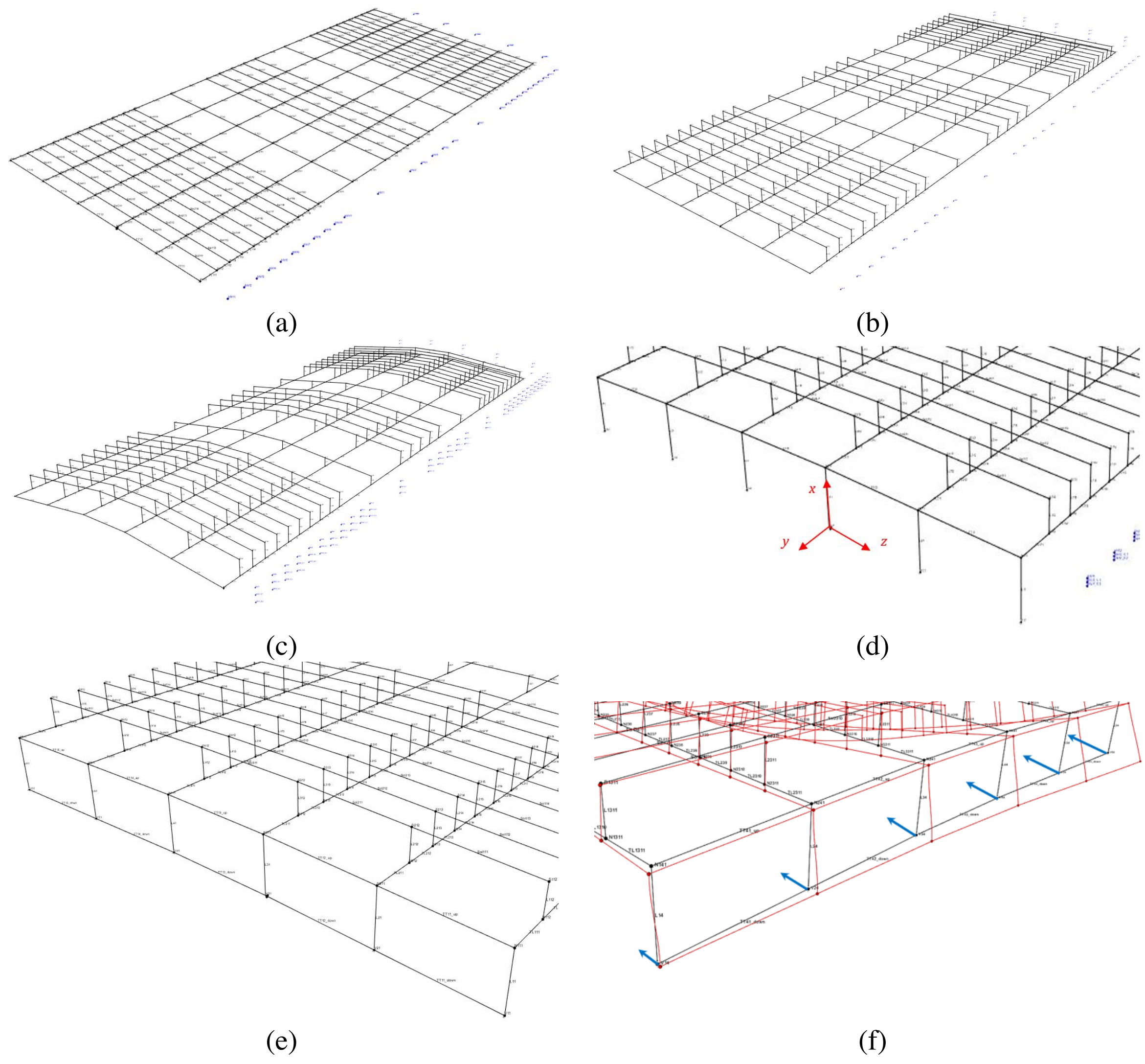

(a) (b)

(c) (d)

(e) (f)

Figure 5. Different fem models realized: global views and details

Table 4. Numerical vs. experimental rotations

		Rotation [mrad]				Difference from measured values [%]			
Beam number		2	3	4	5	2	3	4	5
Experimental	North	0.53	0.36	0.15	0				
	South	0.52	0.32	0.20	0				
Model 1 (a)		0.66	0.42	0.20	0	25÷27	11÷19	0÷9	0
Model 2 (b)		0.65	0.42	0.20	0	23÷25	11÷19	0÷9	0
Model 3 & 4		0.61	0.39	0.19	0	15÷17	6÷13	-2÷8	0
Model 5		0.60	0.39	0.19	0	13÷15	6÷13	-2÷8	0
Model 6		0.58	0.38	0.20	0	9÷12	4÷12	0÷9	0
Model 7		0.55	0.35	0.17	0	3÷5	-5÷2	-4÷4	0

In Table 5 are presented: the vertical reactions due to the weight of the lorries, the total vertical reactions during the load test, the maximum allowable friction force in longitudinal direction, the effective longitudinal force present in the bearing because of friction and the longitudinal displacement in the south side bearings.

The horizontal resultant due to friction is about 200 kN that is about 30% of the vertical reaction due to the lorries weight. This horizontal force reduces the deformation of the deck leading the differences between numerical and experimental values to less than 5% as shown in Table 4.

It can be therefore concluded that friction within free bearings plays a fundamental role in monitoring of bridge deck and cannot be neglected as it is commonly done in design.

Table 5. Reactions [kN] and displacements [mm] in free longitudinal bearings

Bearing of beam	1	2	3	4	5	6
Vertical reactions due to lorry weight	298	228	130	65	6	-46
Total vertical reactions during test	1468	1398	1300	1235	1176	1124
Maximum allowable friction force	73	70	65	62	59	56
Effective friction force	73	70	65	62	-13	-56
Bearing long. displacement	1.52	1.12	0.70	0.32	0	-0.33

5. Long term monitoring issues

Long term monitoring has been done on the bridge for six months. A complete description of this experience will be presented in a future paper.

The most relevant issues related to this experience are: the effect of temperature variation on the instruments, the effect of temperature variation of the structure, the creation of a common starting point for all the sensors.

Even if the monitoring system is sold as “temperature compensated” a relevant dependency of the data on temperature was found. Two levels of temperature dependency could be seen: a synchronized one, related to sensors response to temperature variation and a delayed one (of about 6 hours) related to the bridge deck response to temperature.

Two different cleaning operation should therefore be done to obtain rotation measures that are as little dependant on temperature variations as possible: the first taking into account sensors thermal inertia and drift and the second one taking into account the bridge deck thermal properties.

The installation of the system was done with the bridge open to traffic. During installation all sensors cannot be set to a “zero” condition as time goes by between the installation of one instrument and the following, traffic vibrations place the deck in a different deformed position for all sensors and thermal movement are not neglectable between the first and the last instrument to be set. Therefore all instruments begin the monitoring with a different zero condition.

This problem can be solved by registering a zero closing the traffic at night when the load test is performed: before introducing load test lorries, all sensor data are acquired without traffic and the load test ambient temperature is taken as the zero one. All the data registered before test should then be offset in order to have a common starting point.

6. Conclusions

Finite element models suitable for SHM may differ noticeably from the ones used for the design of the same structures. Design operations are oriented to grant a pre-fixed amount of safety with respect to collapse, therefore the models can widely use plasticity theorems and approaches that gran equilibrium of forces but often disregard deformation compatibility.

SHM, on the contrary, is commonly performed when the structure is subjected to ordinary service loads that are hopefully much lower than collapse ones. Following the structural behaviour in service is in many cases by far more complicated than predicting the failure load. Many mechanisms that can be fully neglected at ultimate limit states, like friction inside bearings or tensile strength of concrete may play an important role in determining the structural behaviour in service conditions.

The development of a finite element model for the SHM of a prestressed bridge deck is presented in this paper. The model is realized using only simple 3D beams elements, without the need to use two dimensional plates or shells elements or 3D solid elements. This choice is very important with a view to the scalability of a monitoring campaign.

Nowadays large scale permanent monitoring systems are becoming a standard in the business. The availability on the market of low-cost sensors, broadband internet communication and cloud computing has opened the doors to a massive use of monitoring systems on a large numbers of infrastructures.

When dealing with such numbers of structures, the realization of sophisticated f.e.m. becomes a bottleneck in the procedure as it is a time consuming operation and it need both structural specialists and expensive dedicated software. On the contrary, if simple and light models can be used the overall process receives a doubtless benefit.

The model proposed for the bridge deck studied in this paper is developed through several sophistication steps from the simplest approach to a more complicated one. The results are compared to measured values during load test and the following conclusions can be drawn:

- The correct evaluation of the collaboration width of the flange of transverse beams is a key parameter. The effective span to of the transverse beams to be used in this procedure is not the interaxis between the longitudinal beams, but it may be close to the transverse width of the whole deck. Longitudinal beams provide, in fact, a kind of vertical elastic restraint to transverse ones, which is by far less stiff than a rigid one.
- The vertical eccentricity of the bearings positions with respect to the longitudinal beams axis should be also modelled with care as it plays a fundamental role if friction in the free bearings should be considered. The model of the first and last transverse beam, that are connecting the bearings should be different from the one used for the transverse placed along the span, to take into consideration the correct level of restraint.
- Friction in free bearings can play a determinant role in modifying the deformability of the structure. Being friction a non-linear behaviour it may complicate remarkably the model, shifting it from elastic linear to non linear and therefore avoiding to use the simple superposition of effect law that is very useful in ordinary design. Rigid perfectly plastic friction model was used in this work, but a simplification of this behaviour using linear spring is under study.
- The deck is prestressed both longitudinally and transversely, therefore linear elastic behaviour under service load is a verified hypothesis. Modelling not prestressed decks may become more difficult if cracking issues can affect the deformation in a non-linear way.

References

[1] L. C. Neves, D. M. Frangopol, “Condition, safety and cost profiles for deteriorating structures with emphasis on bridges”, *Reliability Engineering & System Safety*, Vol. 89, n. 2, pp. 185-198, 2005.
[2] G. Bertagnoli, M. Malavisi, G. Mancini, “Large scale monitoring system for existing structures and infrastructures” 4th World Multidisciplinary Civil Engineering-Architecture-Urban Planning Symposium, WMCAUS 2019 (IOP Conference series: Materials science and Engineering – vol. 603 Section 5) Prague, 17–21 June 2019, 052042.
[3] G. Bertagnoli, F. Luca, M. Malavisi, D. Melpignano, A. Cigada, “A large scale SHM system: A case study on pre-stressed bridge and cloud architecture”. *Pakzad S. (eds) Dynamics of Civil Structures, Volume 2. Conference Proceedings of the Society for Experimental Mechanics Series.*, pp. 75-83, 2020.
[4] C. R. Farrar, K. Worden, “Structural Health Monitoring, a Machine Learning Perspective”, John Wiley & Sons, ISBN: 978-1-119-99433-6, 2013.
[5] C. J. A. Tokognon, B. Gao, G. Y. Tian, Y. Yan, “Structural health monitoring framework based on internet of things: a survey”. *IEEE Internet of Things J.*, vol.7(4), pp. 619-635, 2017.
[6] A. Cigada, F. Lucà, M. Malavisi, G. Mancini, “A Damage Detection Strategy on Bridge External Tendons Through Long-Time Monitoring”, *Pakzad S. (eds) Dynamics of Civil Structures, Volume 2. Conference Proceedings of the Society for Experimental Mechanics Series. Springer,* pp. 159-168, 2021.
[7] A. Cigada, F. Lucà, M. Malavisi, G. Mancini, “Structural health monitoring of a damaged operating bridge: Asupervised learning case study”, *Pakzad S. (eds) Dynamics of Civil Structures, Volume 2. Conference Proceedings of the Society for Experimental Mechanics Series. Springer,* pp. 169-177, 2021.
[8] *fib* Bulletin N°15: Durability of post-tensioning tendons : proceedings of a workshop held at Ghent University on 15-16 November 2001, Lausanne, 2001.
[9] D. Gino, P. Castaldo, G. Bertagnoli, L. Giordano, G. Mancini, “Partial factor methods for existing structures according to fib Bulletin 80: Assessment of an existing prestressed concrete bridge”, *Structural Concrete*, Vol. 21, n.1, pp. 15-31, 2020.
[10] P. Castaldo, G. Amendola, “Optimal DCFP bearing properties and seismic performance assessment in nondimensional form for isolated bridges”, *Earthquake Engineering and Structural Dynamics*, https://doi.org/10.1002/eqe.3454 , 2021.
[11] P. Castaldo, M. Ripani, R. L. Priore, “Influence of soil conditions on the optimal sliding friction coefficient for isolated bridges”, *Soil dynamics and hearthquake engineering*, vol.111, pp. 131-148, 2018.
[12] https://www.raspberrypi.org/documentation/ last acces on 20/04/2021
[13] *fib* Bulletin N°45: Practitioner’s guide to finite element modelling of reinforced concrete structures – State of the art report, Lausanne, 2008.
[14] CEN. EN 1992-1-1: Eurocode 2 – Design of concrete structures. Part 1-1: general rules and rules for buildings, CEN 2014, Brussels, 2014.